



## NANO-CERAMIC CONDUCTING GLASSES : PREPARATION AND PROPERTIES

R. V. BARDE\* and S. A. WAGHULEY<sup>a</sup>

Dept. of Engg. Physics, H.V.P.M. College of Engg. & Technology, AMRAVATI – 444601 (M.S.) INDIA

<sup>a</sup>Department of Physics, Sant Gadge Baba Amravati University, AMRAVATI – 444602 (M.S.) INDIA

(Received : 21.02.2012; Revised : 15.03.2012; Accepted : 21.03.2012)

### ABSTRACT

The nano-ceramic conducting glasses have possessed technological importance because of their simple composition and strong glass forming characteristics. Several effective approaches have been made to enhance the ionic conductivity and chemical durability of the alkali ion conducting binary phosphate glasses, which include the addition of another glass former, modifier oxide and alkali metal halides. The nano-ceramic glasses are synthesized by conventional quenching technique with nano ceramic as dopant materials. The nanodopants may improve the physical properties of conducting glass. All the molten samples were cast in to a carbon plate in air and annealed at 260°C to remove thermal stresses for 3 h and then very slowly cooled to room temperature. XRD patterns of the alloy containing nano-composites with the base glass have anamorphous nature. The variation in electrical conductivity with temperature may be explained by change in the nano-particles (NPs) ions. The spectroscopical study reveals that the plasmon bands are slowly shifted and depending on increasing ratio of nano-particles (NPs).

**Key words:** Synthesis, Physical Properties, Nano-ceramics, conducting glass.

### INTRODUCTION

Nano-ceramics are nano scale particles or structures consisting of ceramic materials. Nano-ceramics include oxide and non-oxide materials. Nano-ceramics describe a relatively large family of various materials with different properties and application. The main part of nano-ceramic materials is consisting of oxide ceramics. Various nano-scale metal oxides are currently investigated for different applications and in more or less advanced research state viz. Indium-Tin oxide (ITO), Aluminium oxide ( $Al_2O_3$ ), Silicon dioxide ( $SiO_2$ ), Titanium oxide ( $TiO_2$ ), Zinc oxide (ZnO), Zirconium and cerium oxides, Iron oxide etc.<sup>1</sup>

Rare-earth (RE)-doped glasses has an important category of photonic materials with their range of applications of extending from light energy conversion (up and down conversions) to detection, optical communications, random lasers, biomedical lasers, information processing, display technology, etc.<sup>2-4</sup> The presence of plasmonic metal nano-particles (NPs) in the vicinity of luminescent RE ions affects the RE-luminescence and creates exciting opportunities for the development of new technologies<sup>5,6</sup>. Nano-metal-enhanced luminescence, (NMEL) or radiative decay engineering has already emerged as a powerful tool in biotechnology and in inorganic transparent glasses<sup>7</sup>. It is presently finding ever-increasing applications in

newly emerging Plasmon controlled nano-photonics technologies like solar cells, light emitting diodes, advanced displays, high quality optical communication systems, etc.<sup>8,9</sup> The enhanced local field properties of plasmonic nano-particles (NPs) have recently been used to design Plasmon enhanced dye sensitized solar cell<sup>10,11</sup>.

The glass based nano composites is transparent materials; they can be easily fabricated to adapt solar cell designs as cover plates or as backside coatings. The spatially localized enhanced electric field around the metallic nanostructures arises due to the mismatch between the dielectric function of the metallic nano-particles (NPs) and the host glass<sup>12-14</sup>. Larger nano-particles (NPs) may enhance luminescence due to the increased contribution of nano particle scattering<sup>15,16</sup>. Nano-metal-enhanced luminescence, (NMEL) or metal induced radiative decay rate enhancement also depend on nano particle separation. Very short distance leads to quenching due to creation of new non radiative channels due to light absorption inside the metal and energy transfer from the excited state of the rare-earth ion to the surface Plasmon's of the metal surface<sup>17,18</sup>. Hence, there must exist an optimum separation distance for maximum emission enhancement.

The use of silver as a luminescence sensitizer of rare earth ions in the glasses is encouraged because the small absorption cross sections have afforded the attempts to increase the excitation efficiency of these ions<sup>19,20</sup>. The heat stability of ITO conducting glass was greatly improved by depositing metal oxide, such as antimony-doped tin oxide (ATO), aluminum doped zinc oxide, and SnO<sub>2</sub>, on the ITO layer. The cell made from mesoporous assembled TiO<sub>2</sub> nano crystal (MP-TiO<sub>2</sub>) showed the higher cell efficiency (6.5%) than that made from commercially available P<sub>2</sub>O<sub>5</sub> TiO<sub>2</sub> powders (5.6%). Gold doped ruby glasses are classical examples of metal-glass nano composites that have been investigated for their striking optical properties and for their multifunctional applications<sup>22</sup>.

## Synthesis

Tirtha et al.<sup>23</sup> reported that Potassium Meta borate, antimony (III) oxide, chloroauric acid, silver nitrate, and neodymium (III) oxide were the raw materials. The base glass (20 g) of composition (mol %) 15K<sub>2</sub>O–15B<sub>2</sub>O<sub>3</sub>– 70Sb<sub>2</sub>O<sub>3</sub> (KBS) was melted in a high purity silica crucible at 900°C in a raising hearth electric furnace using these raw materials. To prepare the nano composites, all the dopants were used in excess. All the molten samples were cast in to a carbon plate in air and annealed at 260°C to remove thermal stresses for 3h and then very slowly cooled to room temperature. The schematics of the synthesis are shown in Fig. 1. Samples of about 2.0±0.01 mm thicknesses were polished for optical measurements. The density of the glasses was measured by Archimedes method using toluene as buoyancy liquid with an error of ± 0.7%. The UV–Vis–NIR absorption spectra were recorded using a Lambda 20 double-beam spectrophotometer (Perkin-Elmer) at an error of ± 0.1 nm. The X-ray diffraction patterns of the bulk samples were recorded with the step time 0.5 s, from 101 to 801. TEM was done using a Jeol JEM2010 operating at 200kV. Fluorescence spectra were measured, at ± 0.2 nm error, with a Fluorolog 2 fluorescence spectrophotometer with a Xe lamp as excitation source and a photomultiplier tube as detector. The excitation slit (1.25 mm) and emission slit (0.5 mm) were kept same for all samples. All measurements were carried out at room temperature. The enhancement of luminescence was found to be reproducible for all samples.

Giehl et al.<sup>24</sup> reported that the glass samples were prepared by melt-quenching method using appropriately weighed high-purity compounds: TeO<sub>2</sub>, Na<sub>2</sub>CO<sub>3</sub>, ZnO and AgNO<sub>3</sub>. The batches were held at the temperature of 850 °C at an electric furnace, in air, during 30 min in platinum crucible. The thermograms of the differential thermal analysis (DTA) were obtained with the model DTA-50 of Shimadzu equipment at the heating rate of 10°C/s and the values of glass transition (T<sub>g</sub>) crystallization (T<sub>c</sub>) and melting (T<sub>m</sub>) temperatures determine. The optical absorption (OA) was performed with the model 500 double-beam Cary spectrophotometer in the absorbance mode, in the wavelength range of 200–3000 nm. The morphology of

the precipitated nano particles was studied from the transmission electron microscope (TEM) Philips model CM 200, operating at 200 kV. The refractive indices were performed at room temperature using the Metricon Model 2010 equipment containing three laser light sources of wavelengths 632.8, 1305 and 1536 nm, respectively, which allows the refractive indices measurements with precision of 0.0002. The densities were determined using the Archimedes method, with precision of 0.0001 g, with distilled water as the immersion fluid.

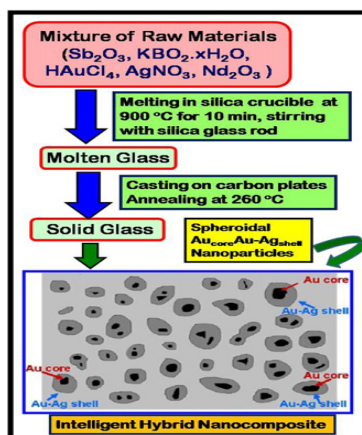


**Fig. 1: Schematics of single-step nano composite synthesis**<sup>23</sup>

Pietrzaka et al.<sup>25</sup> reported that an electronically conducting nano material was synthesized by nano crystallization of a  $90\text{V}_2\text{O}_5 \cdot 10\text{P}_2\text{O}_5$  glass and its electrical properties were studied in an extended temperature range from  $-170$  to  $+400^\circ\text{C}$ . The conductivity of the prepared nano material reaches  $2 \times 10^{-1} \text{ S cm}^{-1}$  at  $400^\circ\text{C}$  and  $2 \times 10^{-3} \text{ S cm}^{-1}$  at room temperature. It is higher than that of the original glass by a factor of 25 at room temperature and more than 100 below  $-80^\circ\text{C}$ . The observed conductivity dependencies are discussed in terms of the Mott's theory of the electronic hopping transport in disordered systems. Since  $\text{V}_2\text{O}_5$  is known for its ability to intercalate lithium, the presented results might be helpful in the development of cathode materials for Li-ion batteries.

Uma et al.<sup>26</sup> reported that high-proton-conducting  $\text{P}_2\text{O}_5\text{-SiO}_2\text{-PWA}$  glasses were prepared at  $600^\circ\text{C}$  and they were characterized as a function of  $\text{P}_2\text{O}_5$  and PWA. TG/DTA measurements were carried out with the model SSC-5200 under a nitrogen atmosphere using heating rate of  $5^\circ\text{C}/\text{min}$ . Fourier transform infrared (FTIR) spectra of glasses were collected using an FTIR spectrometer in the range  $400\text{-}4000 \text{ cm}^{-1}$ . The average pore diameter was measured from gas adsorption analyzer. The pore-size distribution was established using the BJH method and specific surface areas were determined by the BET method. Proton conductivity of the  $\text{P}_2\text{O}_5\text{-SiO}_2\text{-PWA}$  glass was evaluated by the ac impedance method between 0.1 Hz to 1 MHz using an impedance analyzer. Electrochemical measurements were made at  $30^\circ\text{C}$  and relative humidity 30% with a Solartron 1286, electrochemical interface, and 1287 frequency response analyzer. The maximum power density value of  $15.5 \text{ mW}/\text{cm}^2$  was attained at  $30^\circ\text{C}$  with 30% humidity. The fuel-cell performance could be further improved by optimization of electrode/electrolyte compositions with different operating conditions.

### Physical properties

The X-ray diffraction can be used to estimate the average crystallite sizes. XRD patterns of the alloy containing nano-composites with the base glass have an amorphous nature. The XRD diffraction peaks are fairly weak because the concentration of the nano-metal embedded within bulk amorphous glass matrix is very low.

The variation in electrical conductivity with temperature may be explained by change in the nano-particles (NPs) ions. The doping of nano-particles (NPs) ions improves the electrical properties. The temperature dependence of DC electrical conductivity has been studied in terms of different hopping models.

The density is found to increase gradually with increase in dopant concentration. They showed uniform intense coloration manifesting almost homogeneous distribution of the nano-particles (NPs) in the composite network indicating their possible use as ornamental items as well. The progressive change in color of the nano-composites is attributed to the different Au and Ag concentration ratios, which lead to the shift of the SPR band frequency in the visible region<sup>23</sup>. A transmission electron microscopy (TEM) image of the nano-composite showed the formation of core shell nanostructures with sizes varying from 22 to 107 nm. The TEM images of bimetallic Ag and Au core shell nano-particles (NPs) are known to display areas of contrasting density with the dark region attributable to gold and the light region attributable to silver<sup>27</sup>.

UV-Vis-NIR absorption spectroscopy shows that the Plasmon bands are slowly shifted and depending on increasing ratio of nano-particles (NPs). The UV-vis absorption spectra also show characteristic absorption peaks of nano-particles (NPs) ions. The photoluminescence up conversion of nano-particles (NPs) excited at 805 nm show two prominent up conversion peaks. Significant enhancement of both the fluorescence peaks was observed in the presence of bimetallic nano-particles (NPs). The values of the densities and refractive indices at different wavelengths were found out. From the reading it is seen that the densities and refractive indices increase with increasing the nano-particles (NPs). Rare earth ions triply doped glasses have been showed the infrared to visible up conversion emissions under 980 nm laser diode excitation at room temperature.

### **Applications**

There are various applications of nano-particles (NPs) ions doped conducting glasses viz. light energy conversion (up and down conversions) to detection, optical communications, random lasers, biomedical lasers, information processing, display technology, etc. Presently it find ever-increasing applications in newly emerging Plasmon controlled nano-photonics technologies like solar cells, light emitting diodes etc. It is used to design Plasmon enhanced dye sensitized solar cell.

### **CONCLUSION**

The nano-ceramic glasses are synthesized by conventional quenching technique with nano ceramic as dopant materials. The variation in electrical conductivity with temperature may be explained by change in the nano-particles (NPs) ions. The doping of nano-particles (NPs) ions improves the electrical properties. The temperature dependence of DC electrical conductivity has been studied in terms of different hopping models. XRD patterns of the alloy containing nano-composites with the base glass have an amorphous nature. The XRD diffraction peaks are fairly weak because the concentration of the nano-metal embedded within bulk amorphous glass matrix is very low. UV-Vis-NIR absorption spectroscopy showed that the Plasmon bands are slowly shifted and depending on increasing ratio of nano-particles (NPs) and characteristic absorption peaks of nano-particles (NPs) ions. There are various applications of nano-particles (NPs) ions doped conducting glasses.

### **ACKNOWLEDGEMENT**

Authors are thankful to Head, Department of Physics Sant Gadge Baba Amravati University, Amravati for providing necessary facilities.

**REFERENCES**

1. B. Basu, *Current Science (Bulletin)*, **95** (2008).
2. C. H. Kam, S. Buddhudu, *J. Quant Spectrosc Radiat Transfer.*, **85**, 1-12 (2004).
3. C. H. Kam, S. Buddhudu, *J. Quant Spectrosc. Radiat. Transfer.*, **87**, 325-37 (2004).
4. Z. Dai, A. Fang, *J. Quant Spectrosc. Radiat. Transfer.*, **101**, 226-36 (2006).
5. S. M. Lee, K. C. Choi, *Opt. Express*, **18**, 12144-52 (2010).
6. M. A. Noginov, G. Zhu, C. Davison, A. K. Pradhan, K. Zhang, M. Bahoura, *J. Mod. Opt.*, **52**, 2331-41 (2005).
7. C. D. Geddes, J. R. Lakowicz, *J. Fluoresc.*, **12**, 121-9 (2002).
8. P. N. Prasad, *Nano Photonics*, New Jersey: Wiley, 129-51 (2004).
9. J. Z. Zhang, *World Scientific Publishing Co. Pte. Ltd.* (2009).
10. M. D. Brown, T. Suteewong, R. S. S. Kumar, V. D'Innocenzo, A. Petrozza, M. M. Lee, *Nano Lett.*, **1**, 438-45 (2011).
11. S. D. Standridge, G. C. Schatz, J. T. Hupp, *J. Am. Chem. Soc.*, **131**, 8407-9 (2009).
12. S. A. Marier, H. A. Atwater, *J. Appl. Phys.*, **98**, 011101, 10 (2005).
13. V. M. Shalaev, S. Kawata, *Elsevier* (2007).
14. F. Lee, D. W. Brandl, Y. A. Urzhumov, H. Wang, J. Kundu, N. J. Halas, *ACS Nano*, **2**, 707-18 (2008).
15. F. Tam, G. P. Goodrich, B. R. Johnson, N. J. Halas, *Nano Lett.*, **7**, 496-501 (2007).
16. J. W. Liaw, C. S. Chen, J. H. Chen, *J. Quant Spectrosc. Radiat. Transfer.*, **111**, 454-65 (2010).
17. M. Eichelbaum, K. Rademann, *Adv. Funct. Mater.*, **19**, 1-8 (2009).
18. H. Nabika, S. Deki, *J. Phys. Chem.*, **B107**, 9161-4 (2003).
19. C. Strohhofer, A. Polman, *Silver As a Sensitizer for Erbium*, *J. Appl. Phys.*, **81**, 1414 (2000).
20. L. R. P. Kassab, C. B. De Araújo, R. A. Kobayashi, R. A. Pinto, D. M. Da Silva, *J. Appl. Phys.*, **105**, 103505 (2009).
21. D. Pliszkaa, B. Kuszab, M. Gazdab, (2011), *Solid State Ionics*, **192**, 210-214.
22. S. Tirtha, B. Karmakar, *J. Quantitative Spectroscopy & Radiative Transfer*, **112**, 2469-2479 (2011).
23. J. M. Giehl, W. M. Pontuschka, L. C. Barbosa, E. F. Chilloce, Z. M. Da Costa, S. Alves, *Optical Materials*, **33**, 1884-1891 (2011).
24. T. K. Pietrzaka, J. E. Garbarczyka, M. Wasiucionecka, I. Gorzkowskab, J. L. Nowinskia, S. Gierlotkac, *J. Power Sources*, **194**, 73-80 (2009).
25. T. Uma, M. Nogami, *Ionics*, **12**, 167-173 (2006).
26. I. Srnova-Sloufova, F. Lednický, A. Gemperle, Gemperlova, *J. Langmuir*, **16**, 9928-35 (2000).